Active magnetic bearings - chances and limitations

Schweitzer G

International Centre for Magnetic Bearings, ETH Zurich, CH-8092 Zurich, schweitzer@ifr.mavt.ethz.ch

Magnetic bearings are increasingly being used for a large variety of applications. Their unique features make them attractive for solving classical rotor-bearing problems in a new way and allow novel design approaches for rotating machinery. Classical limitations can be overcome and feature ranges can be extended. Of course, limitations still hold, imposed by principally valid physical constraints and by the actual state of the art. In order to facilitate design decisions this paper describes such limitations.

1. Introduction

Initially, three decades ago, active magnetic bearings (AMB) have been designed to overcome the deficiencies of conventional journal or ball bearings. Mostly in research labs, they showed their ability to work in vacuum with no lubrication and no contamination, or to run at high speed, and to shape novel rotor dynamics. Today, magnetic bearings have been introduced into the industrial world as a very valuable machine element with quite a number of novel features, and with a vast range of diverse applications. Now, there are questions coming up about the actual potential of these bearings: what experiences have been made as to the performance, what is the state of the art, what are the physical limits, what can we expect? In particular, there are features such as *load, size, stiffness, temperature, precision, speed, losses and dynamics*. Even such complex issues as reliability and smartness of the bearing can be seen as features, with increasing importance and growing maturity. The paper will discuss key problems and give application examples. It will help to make design decisions, point to alternatives to classical approaches, and in the end, it might stimulate further research into promising areas.

2. Load

The term *load* already, as simple as it seems, touches upon basic properties of magnetic bearings. The load capacity depends on the arrangement and geometry of the electromagnets, the magnetic properties of the material, of the power electronics, and of the control laws - a set-up with main elements is shown in Figure 1. Furthermore, carrying a load is not just a static behaviour – usually it has strong dynamic requirements. Subsequently, first the static properties of an AMB and the generation of magnetic forces will be briefly outlined [1].

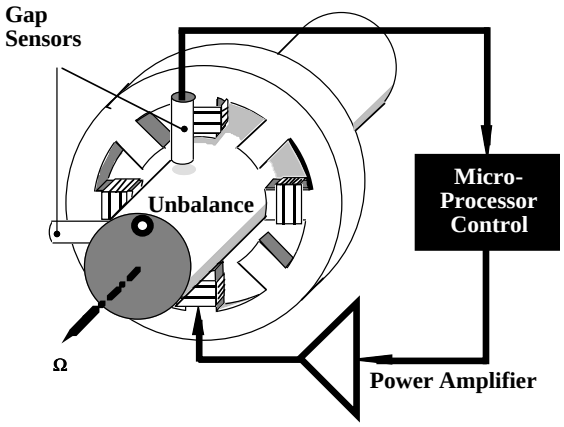

Figure 1. Basic set-up of an active magnetic bearing carrying a rotor load

Magnetic forces are generated in magnetic fields. Magnetic fields themselves can be generated by a current, or a permanent magnet. For example, a rotation-symmetrical *magnetic field* $\boldsymbol{H}$ is generated around a straight conductor with a constant current i (Figure 2a). The contour integral around the conductor says that

$$\oint \boldsymbol{H}\,\mathrm{d}s = i \tag{1}$$

This means that the magnitude of the magnetic field in Figure 2a is $H = i/2\pi r$. The magnetic field is independent of the material around the conductor. If the integration path encompasses several current loops, as is the case with the air coil in Figure 2b, then the integral yields

$$\oint \boldsymbol{H}ds = ni \tag{2}$$

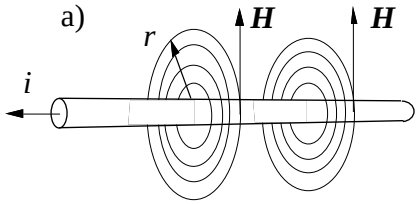

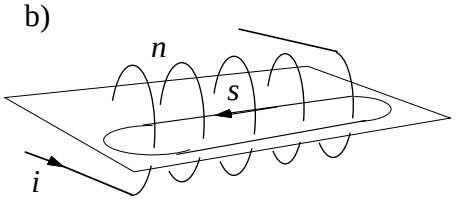

Figure 2. a) Conductor with magnetic field b) Air coil

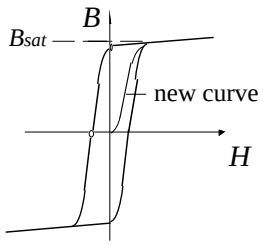

Figure 3. B-H diagram, hysteresis loop, saturation

In magnetic bearing technology electromagnets or permanent magnets cause the magnetic flux to circulate in a magnetic loop. The magnetic flux $\boldsymbol{\Phi}$ can be visualized by magnetic field lines. Each field line is always closed. The density of these lines represents the flux density $\boldsymbol{B}$. The magnetic field $\boldsymbol{H}$ is linked to the *flux density* $\boldsymbol{B}$, ie. *magnetic induction*, by

$$\boldsymbol{B} = \mu_0\,\mu_r(H)\boldsymbol{H} \tag{3}$$

Here, $\mu_0 = 4\,\pi\,10^{-7}$ Vs/Am stands for the *magnetic field constant* of the vacuum, and μ_r is the *relative permeability*depending on the medium the magnetic field acts upon. μ_r equals 1 in a vacuum, and also approximately in air. By using *ferromagnetic material*, where μ_r is generally >>1, the magnetic loop can be concentrated in that core material. The behaviour of ferromagnetic material, is usually visualized in a B-H diagram (Figure 3), showing the well-known phenomena of *hysteresis* and *saturation*. Saturation means, as a consequence, that the flux density $\boldsymbol{B}$ does not increase much more beyond B_{sat} even when the magnetic field $\boldsymbol{H}$ and the generating current i is further increased. The current, corresponding to that saturation limit, be i_{sat}.

For deriving the *force* in an AMB let us consider Figure 4. It shows a single two-pole magnetic bearing element, as part of a complete bearing ring of Figure 1, indicating the path of the magnetic flux $\boldsymbol{\Phi}$.

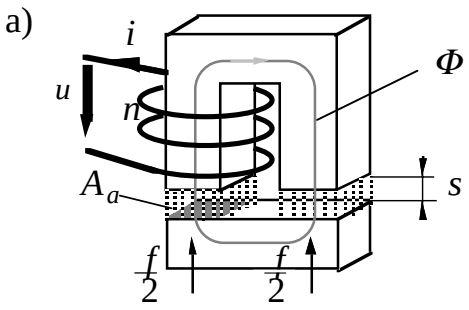

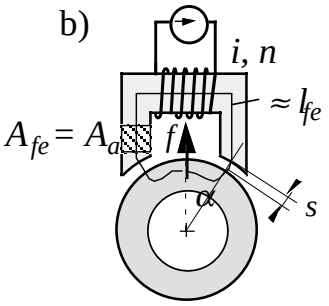

Figure 4. a) Force of a magnet b) Geometry of a radial bearing

The usual assumptions hold, i.e. that the iron part l_{fe} in the magnetic loop is neglected, that the relations for static fields hold as the frequencies for the alternating current are not too high, that the flux Φ is homogeneous in the iron core and the air gap, and that the cross-sectional areas are the same $A_{fe} = A_a$. Then, the induction $B = B_a$ is the same along the magnetic loop. It is proportional to the current i until the saturation induction B_{sat} is reached. A further increase of the current beyond i_{sat} does not increase the induction much further beyond B_{sat}. The force f exerted can be derived by considering the energy W_a stored in the air gap between rotor and magnet

$$W_a = \frac{1}{2} B_a H_a V_a = \frac{1}{2} B_a H_a A_a\, 2s \tag{4}$$

The force acting on the ferromagnetic body is generated by a charge of the field energy in the air gap, as function of the body position. For small displacements ds the magnetic flux $B_a A_a$ remains constant. When the air gap increases by ds the Volume V_a = 2$s$$A_a$ increases, and the energy W_a in the field increases by dW. This energy has to be provided mechanically, i.e. an attractive force has to be overcome. Thus

$$f = \frac{\mathrm{d}W_a}{\mathrm{d}s} = B_a H_a A_a = \frac{B_a^2 A_a}{\mu_0} \tag{5}$$

In the range, where the induction B_a is proportional to the magnetic field H_a and the currrent i, i.e. below saturation, the force as a function of coil current i and air gap s for the arrangement of Figure 4a is

$$f = \mu_0 A_a \left(\frac{n\,i}{2\,s}\right)^2 = \frac{1}{4}\mu_0\, n^2\, A_a \frac{i^2}{s^2} = k\,\frac{i^2}{s^2} \tag{6}$$

Equation (1) shows the quadratic dependence of the force on the current and the inversely quadratic dependence on the air gap. In the case of a real radial bearing magnet, the force of both magnetic poles affect the rotor with an angle α (figure 4b), as opposed to the model of the U-shaped magnet of Figure 4a. In the case of a radial bearing with four pole pairs α equals for instance 22.5°, with cos α = 0.92. Considering α we obtain

$$f = \frac{1}{4}\mu_0\, n^2\, A_a \frac{i^2}{s^2} \cos\alpha = k\,\frac{i^2}{s^2}\cos\alpha \tag{7}$$

The force increases with the maximum admissible "magnetomotive force" ni_{max}, i.e. the product of the maximum current i_{max} and winding number n. This value is subject to design limitations. As a consequence, the maximum value for the force depends on the winding cross section, the mean winding length and the possible heat dissipation, or the available amount of cooling, respectively. Therefore, one limitation for a high static load is the adequate dissipation of the heat generated by the coil current due to the Ohm resistance of the windings. This *"soft" limitation* can be overcome by a suitable design.

Assuming that this problem has been adequately considered, then the current i_{max} will eventually reach a value where the flux generated will cause saturation, and then $i_{max} = i_{sat}$, and the carrying force has reached its maximal value f_{max}. Any overload beyond that physically motivated *"hard" limitation* of the carrying force f_{max} will cause the rotor to break away from its centre position and touch down on its retainer bearings.

In order to compare the carrying performance of different bearing sizes, the carrying force is related to the size of the bearing, or more precisely, to the projection of the bearing area *db* (Figure 5), leading to the *specific carrying force*. Let us assume that the pole shoe width p equals the leg width c. On the bearing diameter d we have one eighth of the circumference per pole at our disposal. Using half of that for the pole shoe width$p$, the pole shoe surface is given by

$$A_a = \frac{d\,\pi}{} 0.5\, b \tag{8}$$

With actually available Si-alloyed transformer sheets, which are used for bearing magnets, a maximum flux density $B_{max} \approx 1.5$ Tesla < B_{sat} is recommended. Inserting this value for B_a in equation (4), and considering that the forces of both poles do not act perpendicularly, but at an angle of π/8, we obtain with A_a from equations (8) and (4) the specific carrying force

$$\frac{f_{max}}{d\,b} = \frac{B_{max}^2\,\pi}{\mu_0\, 8} 0.5 \cos\frac{\pi}{8} = \frac{1.5^2\,\pi}{\mu_0\, 8} 0.5 \cos 22{,}5° = 32\ \frac{\mathrm{N}}{\mathrm{cm}^2} \tag{9}$$

Based on this result, an estimation of the carrying force f_{max} can be determined from Figure 6. The specific load of 32 N/cm^2 (or 0.32 MPa) is considerably lower than that for oil lubricated bearings, which is about four times as high.

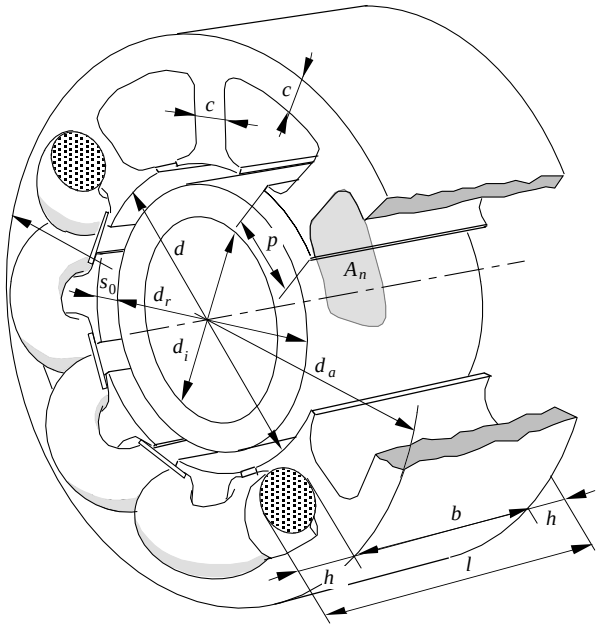

Figure 5. Geometry of a radial bearing magnet, from [2].

d	Inner diameter (bearing diameter	d_a	Outer diameter	d_r	Rotor diameter
c	Leg width	d_i	Shaft diameter	l	Bearing length
h	Winding head height	b	Bearing width (magnetically active part		
A_n	Slot cross section (winding space)	p	Pole shoe width	s_0	Nominal air gap

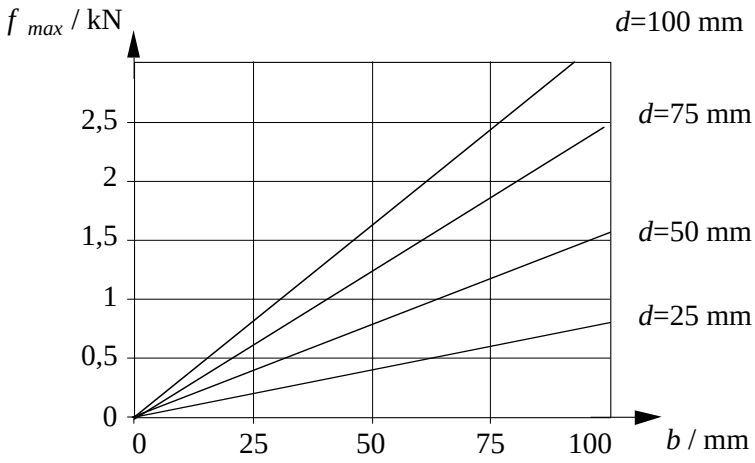

Figure 6. Carrying force of radial bearings having width b and diameter d, at a specific carrying force of 32 N/mm^2.

Using (expensive) cobalt-alloys with a saturation flux density B_{sat} of over 2 Tesla, the magnets can be designed for a flux density of 1.9 Tesla from which a specific carrying force of up to 60 N/cm^2 will result. However, these assessments do not provide any information on the required flux or the space required for the winding, and therefore we do not learn anything about the outer diameter. Often, the entire space requirement of the bearing has to be optimised when designing the bearing magnets, and in many cases the above-mentioned values cannot be achieved because of limited space or extremely wide air gaps.

Examples on high loads, which have been actually realized, include a rotor with a mass of 50 tons (hydropower, axial bearing). The support of rotors for turbo-machinery in gas- and petro-industry with masses in the range of tons is state of the art.

3. Static and dynamic stiffness, bandwidth, actuator power

The stiffness of a bearing characterizes its spring-like behavior, i.e. the ratio of the supported load with respect to the resulting displacement of that load. The term is based on the understanding that a bearing is a mechanical element. In classical bearings the stiffness stems for example from the elasticity of the oil film or the deformation of balls and inner ring of a ball bearing. In an AMB the force is generated by a control current, which can be adjusted to the needs and opens a novel way of shaping the stiffness and even the overall dynamic behavior, and thus the term "stiffness" may not be the best way to describe the performance of an AMB, but is still used for comparison reasons with classical bearings.

One way of obtaining a high *static stiffness* is by applying PID-control. In that way, the current *i*, and implicitly the force as well, is shaped depending on the displacement *x* of the rotor within the air gap as

$$i = Px + I\int x\mathrm{d}t + D\mathrm{d}x/\mathrm{d}t \tag{10}$$

The integral part of the PID control brings the position *x* to the same value before and after the load step, and thus the rotor shows a behavior that cannot be obtained with classical bearings (Figure 7). The time constant for that compensation cannot be made arbitrarily small without increasing the stiffness constant P and the damping constant D. Looking at the bearing only, its static stiffness has become infinite as under stationary load there is no displacement – of course, as long as the maximum carrying force is respected. For comparison, the behavior without compensating integrator is shown, as it would correspond to a classical bearing with spring/damper characteristics as well.

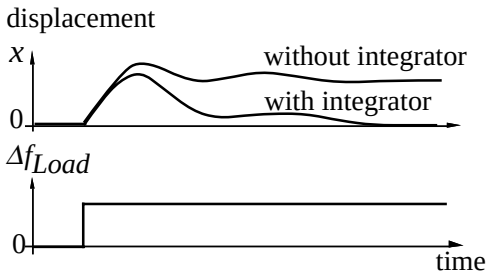

Figure 7. Step response of rotor position to a change in load force with PD and PID control.

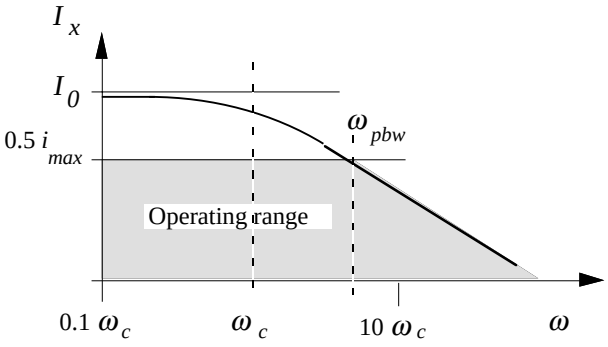

Figure 8. Operating range of a magnetic bearing actuator (power amplifier with bearing magnet)

The term *dynamic stiffness* characterizes the fact that in an AMB the force depends on the control current, and it is frequency dependent, as well as the displacement. There are limitations on the frequency range which will be explained subsequently. The current is generated in a power amplifier, and it makes sense to look at the electromagnet and power amplifier as a unit, the whole unit being termed *magnetic actuator*. The output voltage of the amplifier is limited to a value $\pm U_p$, which is based on the design of the amplifier. If all the voltage is used to overcome the resistance R_{Cu} of the copper windings in the coils a maximum current I_0 can be provided. Figure 8 visualizes the amplitude I_x for the current generated in the bearing windings vs. the frequency ω in the case of an amplifier output voltage $U_p \sin\omega t$. The drop-down at higher frequencies is caused by the inductance *L* of the coils leading to a cut-off frequency $\omega_c = R_{Cu}/L$. If now the amplitude of the current I_x is limited to 0.5 i_{max}, taking into account that usually half of the admissible current i_{max} is being used for pre-magnetization and for carrying constant loads and the other half is being used for generating dynamic forces, we obtain the operating range of the actuator. The highest frequency where the actuator can still operate with its maximal current is called power bandwidth ω_{pbw}. The bandwidth can be enhanced by increasing the power of the amplifier. At higher frequencies the output voltage of the amplifier runs into saturation, and its dynamic behavior becomes nonlinear. The signal bandwidth describes the linear behavior of the actuator and, of course, only holds for the small signal behavior within the operating range The signal bandwidth of the actuator usually goes at least one decade beyond the cut-off frequency ω_c.

When designing a magnetic bearing system one has to estimate the amplifier power P_{max} necessary to achieve the power bandwidth ω_{pbw} for the maximal force amplitude f_{max} over a nominal air gap s_0. It can be shown [1,2], that for a bearing with two magnets, such as in Figure 4b, differentially arranged as in Figure 1, the relation holds

$$\omega_{pbw} = 0.92 \frac{P_{\max}}{s_0 f_{\max}} \tag{11}$$

As an example, a force of 1000N can be generated over an air gap of 0.3 mm with a 1kW amplifier up to a frequency of about 500 Hz. Most of that power is used for the dynamics which can be seen as an inductive load. The actual energy loss, see section on "losses", is much less.

4. Speed

The features characterizing a *high-speed rotor* can be looked at under various aspects. The term "high-speed" can refer to the rotational speed, the circumferential speed of the rotor in a bearing, the circumferential speed of the rotor at its largest diameter, or the fact that a rotor is running well above its first critical bending frequency. The requirements on the AMB and the design limitations can be very different.

Rotational speed

A record from about 50 years ago are the 300 kHz (!) rotation speed that have been realized in physical experiments for testing the material strength of small steel balls (about 1 to 2 mm in diameter) under centrifugal load [3]. In today's industrial applications rotational speeds that have been realized are in the range of about 3kHz for a grinding spindle, or about 5kHz for small turbo-machinery. Problems arise from eddy current and hysteresis losses in the magnetic material, air losses, and the related requirements for power generation and adequate heat dissipation if the rotor runs in vacuum.

Circumferential speed

The circumferential speed is a measure for the centrifugal load and leads to specific requirements on design and material ([4], [1]). The centrifugal load, Figure 9, leads to tangential and radial stresses in the rotor, given by

$$\sigma_t = \frac{1}{8}\rho\,\Omega^2\left[(3+\nu)\,(r_i^2 + r_a^2) + (3+\nu)\frac{r_i^2\,r_a^2}{r^2} - (1+3\nu)\,r^2\right] \qquad \sigma_r = \frac{1}{8}(3+\nu)\,\rho\,\Omega^2\,(r_i^2 + r_a^2 - \frac{r_i^2\,r_a^2}{r^2} - r^2) \tag{12}$$

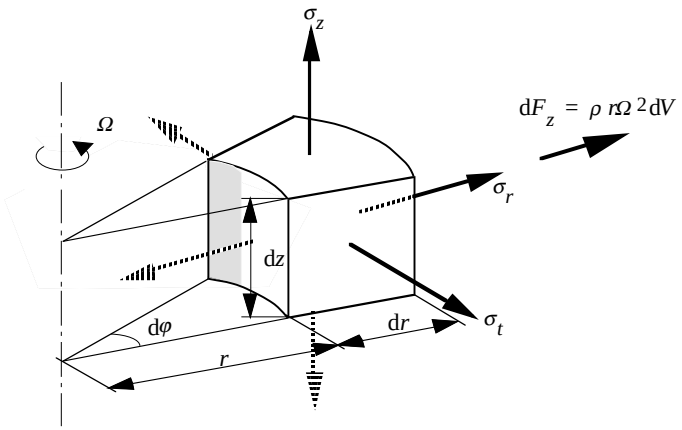

Figure 9. Centrifugal loads acting on the volume element of a rotor

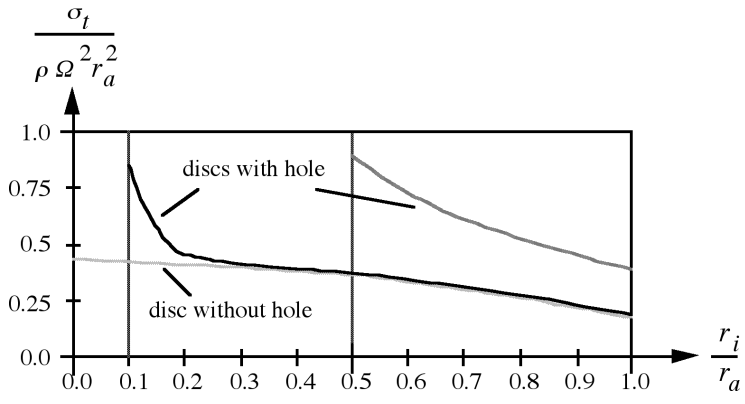

Figure 10. Tangential stress distribution for a disc with and without hole in the centre

The tangential stress, as the most critical one, is shown in Figure 10. Highest stress values occur at the inner boundaries of a rotor disc. As the rotor partially consists of laminated soft iron sheets, which have to be shrink-fit to the rotor shaft, the tangential stress at the inner rim is still further increased. Numerous lab experiments have been performed. Rotor speeds of up to 340 m/s in the bearing area can be reached with iron sheets from amorphous metal (metallic glass), having good magnetic and mechanical properties [4]. The theoretical value for the achievable speed v_{max} lies much higher. It can be derived from Equation 13 (σ_S is the yield strength, ρ is the density of the material), and the according values for some materials are given in Figure 11.

$$v_{max} = (r_a \Omega)_{max} = \sqrt{\frac{8\,\sigma_s}{(3+\nu)\,\rho}} \qquad (13)$$

In industrial applications the speed usually is limited not by the bearings themselves, but by the mechanical design of the motor drive. Figure 12 shows the example of a broken rotor. Figure 13 gives a survey on various AMB applications that have been realized conventionally [5]. For high speeds permanent magnet synchronous drives are used where the rotor is wound with carbon fibres, allowing speeds of about 280 m/s.

Material	v_{max} / [m/sec]
Steel	576
Bronze	434
Aluminium	593
Titanium	695
soft ferromagnetic sheets	565
amorphous metal	826

Figure 11. Achievable circumferential speeds for a full disc

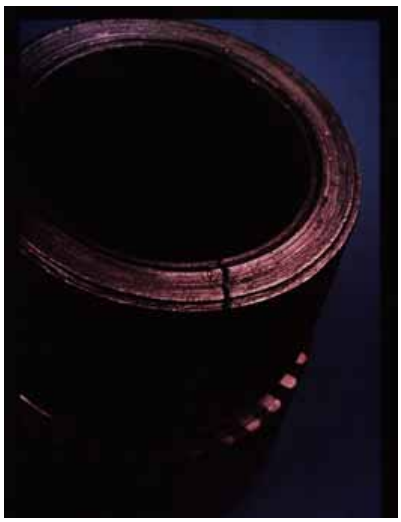

Figure 12. Rotor ring, broken under centrifugal load

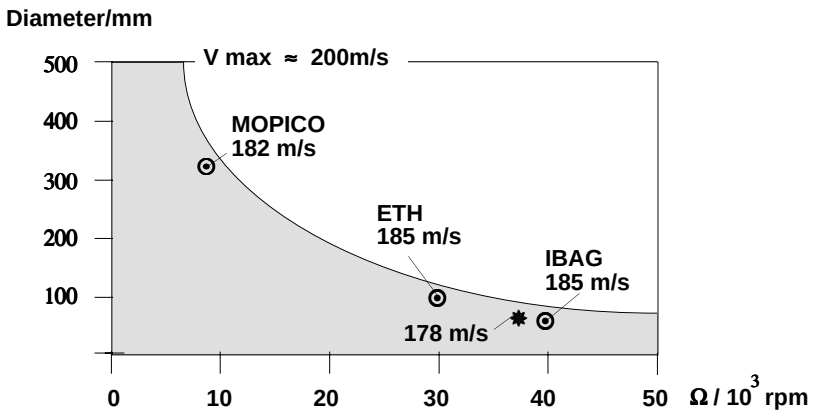

Figure 13. Maximal diameter of the (asynchronous) motor drive in function of the rotor speed (* indicates the rotor of Figure 12 broken at 178 m/s)

Supercritical speed

A rotor may well have to pass one or more critical bending speeds in order to reach its operational rotation speed. In classical rotor dynamics this task is difficult to achieve. In AMB technology it is the controller that has to be designed carefully to enable a stable and well-damped rotor behaviour. Passing just the first critical elastic speed is state of the art and can be very well done with AMB. This has been shown even with an automated controller design, based on self-identification and subsequent self-tuning with the H_∞-method [6]. In many lab experiments two critical speeds have been passed, too, using various design methods, for example [4]. Three elastic modes have been dealt with in [7], using additional notch filters and a zero-pole cancelling filter. It is felt that further research in developing methods for the design of robust control for highly elastic systems is necessary.

4. Size

In principle, there appears to be no upper limit for the bearing size, it can be adapted to any load. Problems arising with assembling the bearing lead to special design variations, where the bearing is separated in two halves, or the single magnets are even treated individually. As an example, Figure 14 shows a large test rig with individual magnets.

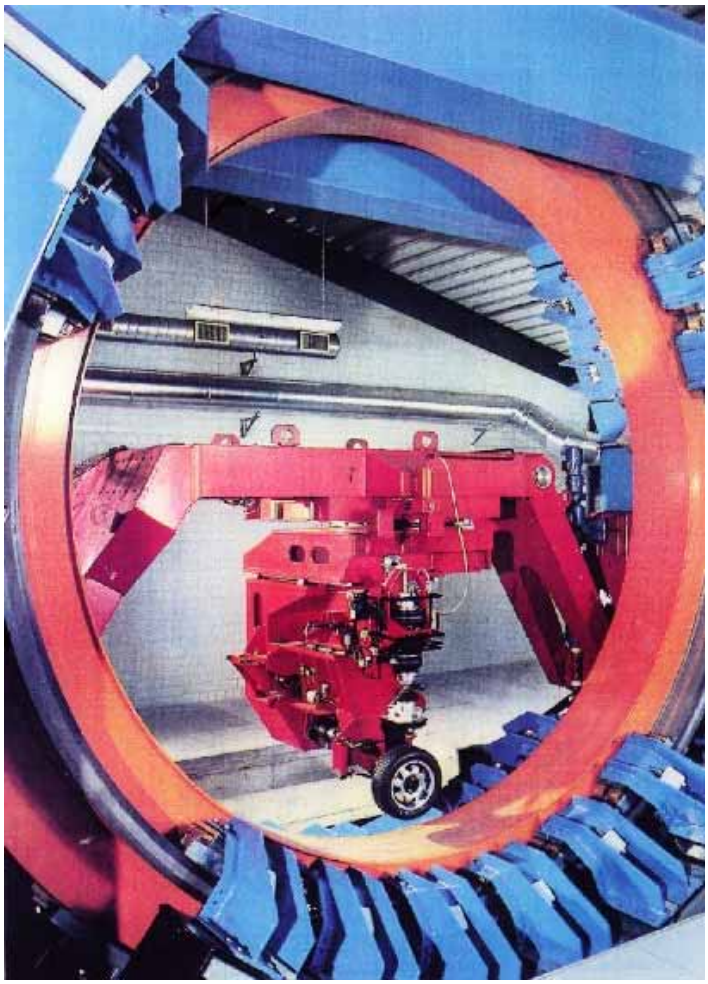

Figure 14. Large test rig for testing high-speed tires, with a magnetically suspended drum representing a road track, using AMB elements from MAGLEV-techniques. Diameter 6m, maximum driving speed 300 km/h

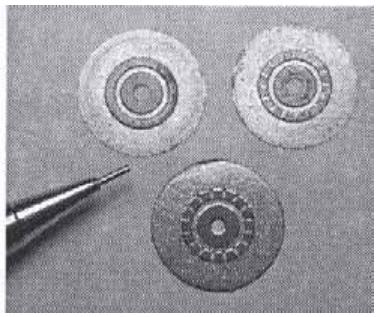

Figure 15. Different designs of three micro-rotors. Diameter 15 mm, thickness 150 to 340 mm, total mass about 270 mg (from [9])

Small bearings are of special interest to micro-techniques. Potential applications are video heads, medical instruments, hard disk drives, and optical scanners. The challenge lies in simplifying the design and in the manufacturing process. Two examples are presented.

In [8] the design, fabrication, and testing of a millimeter-level magnetically suspended micro-motor is described. The micro-motor has a stator outside diameter of 5 mm, rotor outside diameter of 1.5 mm, air gap of 0.1mm, and thickness of 0.5 mm. The stator and rotor are manufactured by both the EDM and UD LIGA methods. The micro-motor with UD LIGA-made rotor has been successfully suspended and spun up to 600 rpm. The proposed micro inductive sensor is made from thick photoresist lithography and electroplating processes has advantages of low cost, good manufacturability, and ease of assembly.

In [9] a very flat micro-motor is presented with an overall thickness of about 2mm, the thickness of the rotor is 150 to 340 mm (Figure 15). It was produced by chemical etching of non grain oriented silicon steel. The air gap is 30 mm. Regarding a future integration of the complete motor with means of thin film technology, inductive sensors were implemented.

5. High Temperature AMB

The application of active magnetic bearings (AMBs) for gas turbines and aircraft engines would open large potentials for novel design. In order to utilize the full advantages of active magnetic bearings, operation in gas turbine and aircraft engines requires that the magnetic bearing should work properly at high temperatures. Challenges in designing such bearings consist in material evaluation, manufacturing process and high temperature displacement sensor development. High temperature active magnetic bearings (HT AMBs) are under development in various places

[10 to 14], Figure 16. Operating temperatures of up to 600 ^{0}C have been reached, at rotor speeds of 50'000 rpm [10]. Such a performance cannot be reached by any other kind of bearing. The soft magnetic materials for stator and rotor are cobalt based alloys [11] such as Hiperco 50 and Hiperco 50-HS, the windings are made of ceramic coated copper wire with high temperature potting materials. Functional tests were quite successful, but the long-term exposure to high temperature needs further research, as the actual results are not yet convincing. In addition, heat dissipation of the internally generated losses under heavy bearing loads have shown to need special attention.

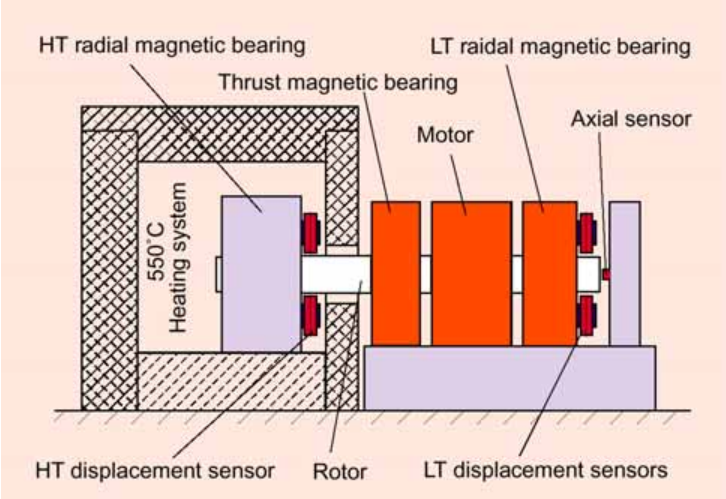

Figure 16. Test rig for a high temperature active magnetic bearing, operating in a containment heated up to 550 ^{0}C, and running at 30'000 rpm. From [14]

6. Losses

With contact-free rotors there is no friction in the magnetic bearings. The operation of active magnetic bearings causes much less losses than operating conventional ball or journal bearings, but, nevertheless, the losses have to be taken into account, and sometimes they lead to limitations [15-22]. Losses can be grouped into losses arising in the stationary parts, in the rotor itself, and losses related to the design of the control.

Losses in the stationary parts of the bearing come mainly from copper losses in the windings of the stator and from losses in the amplifiers. The copper losses are a heat source, and, if no sufficient cooling is provided, can limit the control current and hence the maximal achievable carrying force, as described in section 2.

Losses in the rotor part are more complex and lead to more severe limitations. These losses comprise iron losses caused by hysteresis and eddy currents, and air drag losses. The losses heat up the rotor, cause a breaking torque on the rotor, and have to be compensated by the drive power of the motor. The relations of the various losses with respect to one another are shown in Figure 17. In general, the eddy current losses are the largest ones.

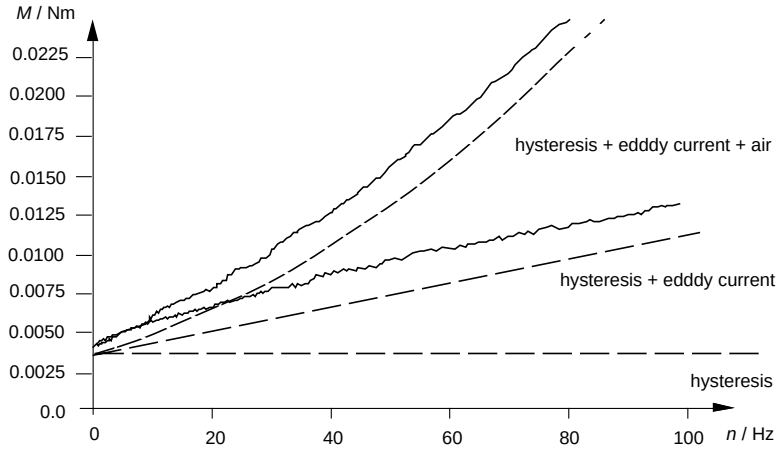

Figure 17. Breaking torques determined from run-down experiments (——) compared to calculated values (---) [2]

The *iron losses* depend on the rotor speed, the material used for the bearing bushes, and the distribution of flux density B over the circumference of the bushes. The breaking torque caused by the iron losses consists of a constant component of hysteresis loss and a component of eddy-current loss, which grow proportionally to the rotational speed. The iron losses in the rotor can limit operations, as, in particular in vacuum applications, it can be difficult to dissipate the generated heat.

The *hysteresis losses* P_h arise if at re-magnetization the B-H-curve in the diagram of Figure 3 travels along a hysteresis loop. At each loop the energy diminishes by $W_h = V_{fe}\, A_{BH}$. Here, A_{BH} stands for the area of the hysteresis loop, and V_{fe} for the volume of the iron. Consequently, the hysteresis losses are proportional to the frequency of re-magnetization f_r. The area of the hysteresis loop depends on the material of the magnet and on the amplitude of the flux density variation. For iron and flux densities between 0.2 and 1.5 Tesla the classical relation

$$P_h = k_h\, f_r\, B_m^{1.6}\, V_{fe} \tag{14}$$

holds, where the material constant k_h has to be derived from loss measurements and from the area of the hysteresis loop, respectively. It is obvious that soft magnetic material with a very small loop area will reduce these losses. Experimentally derived data are presented in [16].

The *eddy-current losses* P_e arise when the flux density within the iron core changes. A compact core (Figure 18a) acts like a short circuit winding and generates large eddy currents. The eddy-current losses can be reduced by dividing the iron core in insulated sheets (figure 18b), or in particles (sinter cores). The smaller these divisions, the smaller the eddy-current losses. Losses in laminated iron can be calculated approximately, if the flux in the sheets is sinusoidal and distributed evenly.

$$P_e = \frac{1}{6\,\rho}\,\pi^2\, e^2\, f_r^2\, B_m^2\, V_{fe} \tag{15}$$

Here, ρ is the specific electric resistance of the iron, e stands for thickness of the sheets, f_r for re-magnetization frequency, and B_m for the maximum flux density or the amplitude of the flux density.

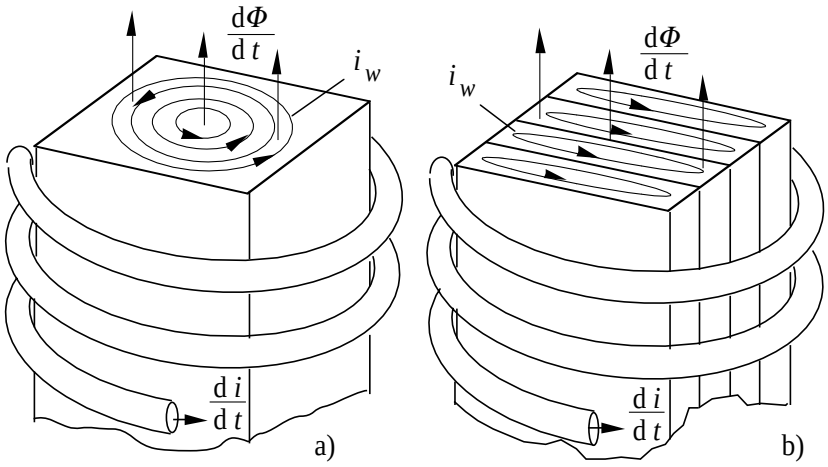

Figure 18. Reducing the eddy current losses by dividing the iron core (a) into sheets (b)

The flux density on the rotor surface, and the inherent losses, depend on the structural shape of the bearing. When the bearing has a format as shown in Figure 19a, the iron is re-magnetized twice upon one revolution. Eddy-current losses can be kept low here since the rotor can be sheeted easily, i.e. built as a stack of punched circular lamination sheets. If, on the contrary, the bearing has a format as shown in Figure 19b, the iron passes below poles with equal polarity, which keeps the hysteresis losses smaller than with format a). However, it is almost impossible to laminate rotor b). Still, the use of format b) is certainly recommended when the rotor needs to be massive, e.g. in high-vacuum applications.

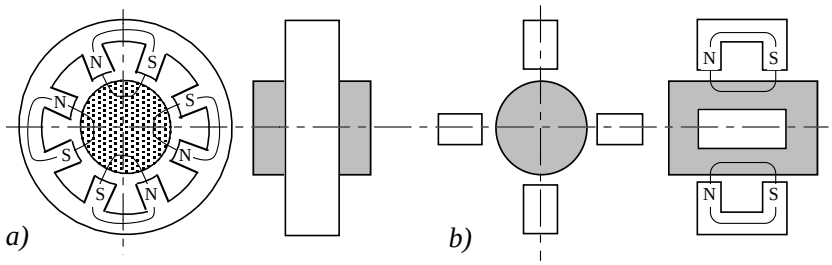

Figure 19. Construction models of radial bearings.
a) Field lines perpendicular to the rotor axis (heteropolar bearing)
b) Field lines parallel to the rotor axis (homopolar bearing)

The use of iron free magnetic bearings and drives, based on Lorentz forces, has been investigated mainly for precision bearings, where the influence of hysteresis would be detrimental to precision control. This approach will be dealt with in the next section under the heading "precision".

The air losses can be predominant at high rotation speeds, and for special applications, such as flywheels for energy storage. They can be calculated or rather estimated by dividing the rotor into sections with similar air-friction conditions, in order to take into account different rotor geometries. Thus, a simple cylindrical rotor is divided, for instance, into cylinders without sheathing, including frontal areas / cylinder front areas within the axial bearing / cylinders within the bearing and the motor / cylinders within the back-up bearing. The breaking torque elements have now to be calculated and then added. Information on how to calculate the breaking torques can be found in [19] and [2]. Very small air gaps increase the air drag.

The *concept of "zero power" control* [20-22] is another way of reducing the losses by reducing the control current itself as much as possible. The static magnetic field, for compensating the static load or for pre-magnetization, is supplied by permanent magnets. The control current is only used for stabilizing the rotor hovering. The rotor is expected to rotate about its main axis of inertia, thus performing a so-called permanent, force-free rotation. The control required for that kind of operation needs information about the periodic parts of the disturbances acting on the rotor, which have to filtered out or compensated for in the sensor signals. The approach is very useful in cases where the energy losses have to be kept minimal, for example for energy flywheels, and where the residual vibratory motions of the geometric rotor axis are not so important.

7. Precision

Precision in rotating machinery means most often how precise can the position of the rotor axis be guaranteed. This has consequences for machining tools, and for the surface quality of parts that are being machined by grinding, milling or turning. In addition, the question of how precise can magnetic bearings become in principle, is of interest for applications such as optical devices, optical scanner, wafer stepper, or lithography. These machines and processes are key elements for semiconductor industry. Active magnetic bearings levitate an object, rotating or not, with feedback control of measured displacement sensor signal. The performance of AMB systems is therefore directly affected by the quality of a sensor signal. Precision control is facilitated by the absence of hysteresis and of deformation-prone heat sources, which touches upon material and design aspects.

The probe type displacement sensors most widely used in AMB system are very sensitive to the surface quality of a rotor, so they require additional algorithms to detect and compensate the unnecessary signal contents induced by the geometric errors of a rotor. Accordingly, on-line control with the probe type sensors becomes more bothersome and more complicated as soon as high precision is aimed at. Algorithms for smoothing out higher order harmonics of geometric rotor errors in the sensor signal, particularly suited for capacitive sensors, have been investigated, for example in [23]. Orbits with rotating errors of 10 to 20 µm have been obtained.

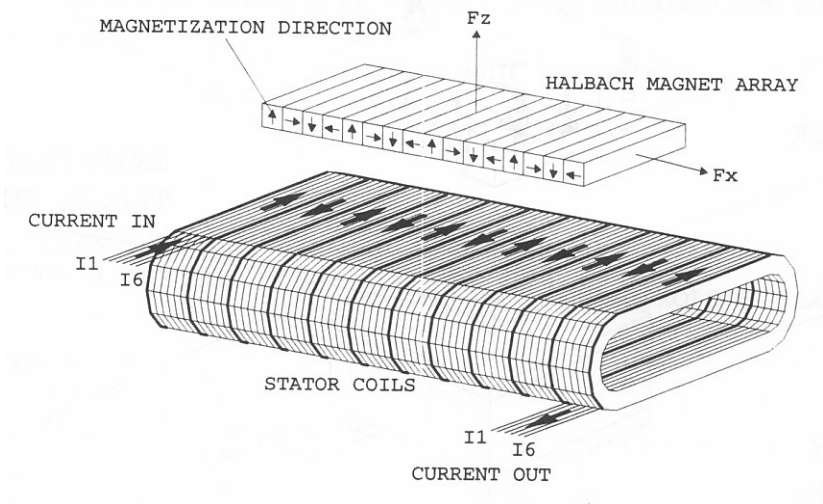

Figure 20. Linear motor configuration for a long-range scanning stage, from [25]

The precision in keeping a hovering position for non-rotating objects has been demonstrated, for example, in [24-26]. For a long-range scanning stage, Figure 20 shows the four linear motors used to suspend and servo the moving element (platen). The stage is used to position samples beneath a scanning-tunneling microscope. Each of the linear motors consists of a stator and a permanent magnet array. Positioned 300 µm directly beneath the magnet array is the stator. The linear motor system is capable of exerting bi-directional vertical and horizontal forces F_Z and F_X as indicated. The platen is light-weighted and floated in oil to reduce bias currents in the motors and to provide viscous damping. The stage has a travel in the horizontal plane of 25 by 25 µm, with 100 µm of vertical travel. Vertical feedback is provided by three capacitance probe sensors while heterodyne laser interferometry is used for lateral position feedback. The stage was designed to have a positioning resolution of 0.1 nm, positioning repeatability of 1nm, and a positioning accuracy of 10 nm.

8. Smart Machine Technology

AMBs are typical *mechatronic devices*, and one of the most attractive features of such devices is their ability of internal information processing. The machine is termed *smart* if it uses its internally measured signals to optimize its state [27]. Such a smart machine makes use of the built-in active control to incorporate additional or higher performance functions. Thus, the machine may acquire higher precision and the ability for self-diagnosis, it can calibrate itself, it can give a prognosis about its future ability to function in a satisfactory way, or about its remaining lifetime, and possibly, it can suggest a correction measure, a therapy, or even induce it itself. It is the mechatronic structure of the machine, the built-in control, its sensors, processors, actuators, and above all, its software which enable these novel features. This is a way to design machines and products with higher performance, less maintenance costs, longer lifetime, and an enhanced customer attraction. In this respect, AMBs already show promising features, but they have by no means reached their full potential. Subsequently an outlook on the concept of such a smart machine is given.

The *smart machine* in Figure 21 consists of three main parts. One is the "Actual Mechatronic System", the actual machine with its process, sensors, actuators and the controller. In our case this would be the rotor of a machine tool or a turbo-machine in magnetic bearings.

The second part is the "Mechatronic System Model", a software representation of the actual machine. Of course, setting up such a model may not be simple, and that is why identification techniques are an important tool in this technology. The model, or a part of it, will be used, too, for designing the control of the actual machine.

The third part describes the "Smart Machine Management". It indicates the additional functions that can be conceived by making "smart" use of the available informations. At first, data have to be collected from the actual machine and its sensors and from the model as well which runs in parallel to the actual machine. Based on this information a diagnosis of the present state will be possible. It can be a model based diagnosis, and furthermore, due to the built-in control loop, self-diagnosis or active diagnosis will be possible, i.e., it will be possible to check assumptions about parameters by creating suitable test signals in the model, and in the actual system. This approach could further improve identification procedures, and it will be of interest for reliability management, for finding out about failures in mechanical components such as cracks in the rotor, or about failures in electrical components, for example in sensors. Based on the results of diagnosis a prognosis about the future behaviour of the machine or about the need for and the consequences of corrective measures can be derived. Such corrections, for example, may be the compensation of an unbalance, special procedures for passing critical speeds, changing the feed of a machine tool during the manufacturing of delicate parts by taking into account the cutting forces or tool wear [29], or it may even lead to a self-tuning of the parameters of the control loop [6].

In particular, the reliability of magnetic bearings, which is one of the most important aspects [30], could be further improved by an appropriate management of the available information and by creating an ana lytical redundancy in addition to any hardware redundancy.

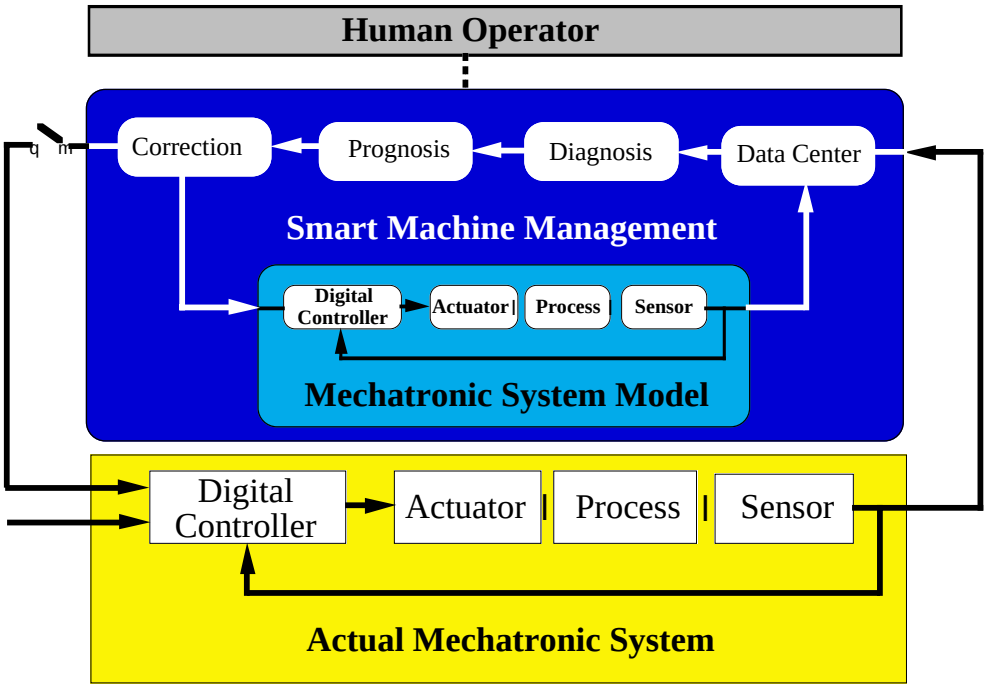

Figure 21. A concept diagram for the structure of a smart machine, from [28]

9. Conclusions

Limitations in Active Magnetic Bearings arise from two reasons: the state of the actual technology in design and material, and from basic physical relations. The paper has given a survey on such limitations, giving a brief theoretical background, showing examples and pointing to actual data. They may help to make substantiated design decisions. The various issues are summarized subsequently:

- the maximal load depend s on design
- the specific load depends on the available ferromagnetic material and its saturation properties, and is therefore limited to 32 to 60 N/cm^2
- the frequency and the amplitude of disturbances acting on the rotor, such as unbalance forces, that can be adequately controlled, depend on the design of the power amplifier (power and bandwidth)
- the maximally achieved rotation speed is about 300 kHz in physical experiments. For industrial applications values of about 6 kHz have been realized
- circumferential speeds, causing centrifugal loads, are limited by the strength of material. Values of about 250 to 300 m/s have been realized with actual design
- supercritical speed means that one or more critical speeds can be passed by the elastic rotor. It appears to be difficult to pass more than two or three
- the size of the bearing depends on design and manufacturability. There are large bearings with dimensions and loads in meters and tons. The smallest bearings actually built have dimensions in the range of mm, with a thickness being as small as 150 μm
- high temperature bearings have been realized, running in experiments at an operating temperature of 600^{o}C (1100^{o}F). For ferromagnetic material the Curie temperature would be a physical limit
- the losses of magnetic bearings at operating speed are much smaller than that of classical bearings. Eddy current losses will limit the rotation frequency of massive rotors (heating up, driving power), the air drag will be crucial at high circumferential speeds (driving power)
- a high precision of the position of the rotor axis (in the range of mm) requires high resolution sensors and adequate signal processing to separate disturbance signals from the desired ones
- a very high precision, aimed at for non rotating suspension and position servoing (in the range of nm), requires iron free magnetic paths to avoid hysteresis effects, and adequate sensing
- the information processing within the AMB system can be used to make the rotating machinery smart. Actual limits have not yet been determined

Further research appears to be indicated in developing insight and outlook at the boundaries of the field of magnetic bearings. A systematic comparison of AMB performance with that of classical bearings needs consistent data. The joint operation of a magnetic bearing with a roller bearing under emergency situations, in load sharing or in touch down contacts, needs further experiments and design efforts. The operation at supercritical speeds, passing many elastic rotor and structure frequencies needs more research on the control design. The advanced information processing within the bearing system, extending the smartness of the rotating machinery, will be a promising research area. The potential and limitations of high temperature super-conductors, as an extension or an alternative to AMBs, is not yet suffiently known.

10. References

[1] Schweitzer G, Bleuler H, Traxler A. (1994) Active Magnetic Bearings, Zurich, vdf Hochschulverlag AG.

[2] Traxler A. (1985) Eigenschaften und Auslegung von beruehrungsfreien elektromagnetischen Lagern. Diss. ETH Zurich Nr. 7851.

[3] Beams JW, Young JL, Moore JW. (1946) The production of high centrifugal fields. J. Appl. Phys., 886-890.

[4] Larsonneur R. (1990) Design and control of active magnetic bearing system for high speed rotation. Diss. ETH Zurich Nr. 9140.

[5] Viggiano F. (1992) Aktive magnetische Lagerung und Rotorkonstruktion elektrischer Hochgeschwindigkeits-antriebe. Diss ETH Zurich Nr. 9746.

[6] Loesch F. (2001) Identification and automated controller design for active magnetic bearing systems. Diss. ETH Zurich Nr. 14474.

[7] Fujiwara H, Matsushita O, Okubo H. (2000) Stability Evaluation of High Frequency Eigen Modes for Active Magnetic Bearing Rotors. *Proc. 7th Internat. Symp. on Magnetic Bearings*, ETH Zurich, August 23-25, 83-88.

[8] Pang DC, Lin JL, Shew BY, Zmood RB. (2000) Design, fabrication, and testing of a millimeter-level magnetically suspended micro-motor. *Proc. 7th Internat. Symp. on Magnetic Bearings*, ETH Zurich, August 23-25, 105-110.

[9] Boletis A, Vuillemin R, Aymon C, Kuemmerle M, Aeschlimann B, Moser R, Bleuler H, Fulin E, Bergqvist J.

(2000) A six magnetic actuators integrated micro-motor. *Proc. 7th Internat. Symp. on Magnetic Bearings, ETH Zurich*, August 23-25, 101-103.

[10] Mekhiche M, Nichols S, Oleksy J, Young J, Kiley J, Havenhill D. (2000) 50 krpm, 1,100°F magnetic bearings for jet turbine engines. *Proc. 7th Internat. Symp. on Magnetic Bearings*, ETH Zurich, August 23-25, 123-128.

[11] Kondoleon AS, Kelleher WP. (2000) Soft magnetic alloys for high temperature radial magnetic bearings. *Proc. 7th Internat. Symp. on Magnetic Bearings*, ETH Zurich, August 23-25, 111-116.

[12] Ohsawa M, Yoshida K, Ninomiya H, Furuya T, Marui E. (1998) High Temperature Blower for Molten Carbonate Fuel Cell Supported by Magnetic Bearings. *Proc. 6th Internat. Symposium on Magnetic Bearings*, MIT Cambridge , August 5-7, 32-41.

[13] Xu L, Zhang J. (2002) A Study on High Temperature Displacement Sensor. To appear in *IEEE Trans. on Instrumentation and Measurement.*

[14] Xu L, Wang L, Schweitzer G. (2000) Development for magnetic bearings for high temperature suspension. *Proc. 7th Internat. Symp. on Magnetic Bearings*, ETH Zurich, August 23-25, 117-123.

[15] Mizuno T, Higuch T. (1994) Experimental measurement of rotational losses in magnetic bearings. *Proc. 4th Internat. Symp. on Magnetic Bearings*, ETH Zurich, August 23-26, 591-595.

[16] Allaire PE, Kasarda MEF, Fujita LK: (1998) Rotor power losses in planar radial magnetic bearings – effects of number of stator poles, air gap thickness, and magnetic flux density. *Proc. 6th Internat. Symp. on Magnetic Bearings*, MIT Cambridge, August 5-7, 383-391.

[17] Meeker D, Maslen E, Kasarda M. (1998) Influence of actuator geometry on rotating losses in heteropolar magnetic bearings. *Proc. 6th Internat. Symp. on Magnetic Bearings*, MIT Cambridge, August 5-7, 392-401.

[18] Ahrens M, Kucera L. (1996) Analytical calculation of fields, forces and losses of a radial magnetic bearing with rotating rotor considering eddy currents. *Proc. 5th Internat. Symp. on Magnetic Bearings*, Kanazawa, August 28-30, 253-258.

[19] Mack M. (1967) Luftreibungsverluste bei elektrischen Maschinen kleiner Baugrössen. Diss. TH Stuttgart.

[20] Fremerey J. K. (1988) Radial Shear Force Permanent Magnet Bearing System with Zero-power axial Control and Passive Radial Damping. In G Schweitzer (Ed) *Magnetic Bearings*, Springer-Verlag, 25-32.

[21] Yakushi K, Koseki T, Sone S. (2000) Three Degree-of-Freedom Zero Power Magnetic Levitation Control by a 4-Pole Type Electromagnet. *Proc. Internat. Power Electronics Conference* IPEC, Tokyo 2000.

[22] Mizuno T. (2000) A unified transfer function approach to control design for virtually zero power magnetic suspension. *Proc. 7th Internat. Symp. on Magnetic Bearings*, ETH Zurich, August 23-25, 117- 123.

[23] Jeon S, Ahn HJ, Han DC. (2000) New Design of Cylindrical Capacitive Sensor for On-line Precision Control of AMB Spindle. *Proc. 7th Internat. Symp. on Magnetic Bearings*, ETH Zurich, August 23-25, 495-500.

[24] Kim WJ, Trumper DL. (1998) Six-degree-of-freedom planar positioner with linear magnetic bearings/motor. *Proc. of the 6th International Symp. on Magnetic Bearings*, MIT Cambridge, 641-649.

[25] Holmes M, Trumper DL, Hocken R. (1998) Magnetically-suspended stage for accurate positioning of large samples in scanned probe microscopy. *Proc. 6th Internat. Symp. on Magnetic Bearings*, MIT Cambridge, August 5-7, 123-132.

[26] Molenaar A, Zaaijer EH, van Beek HF. (1998) A novel low dissipation long stroke planar magnetic suspension and propulsion stage. *Proc. of the 6th International Symp. on Magnetic Bearings*, MIT Cambridge, 650-659.

[27] Schweitzer G. (2000) Magnetic bearings as a component of smart rotating machinery. *Proc. 5th Internat. Conf. on Rotor Dynamics* IFToMM, Darmstadt, Sept. 7-10, 3-15.

[28] Nordmann R, Ewins D, et al. (2001) IMPACT - Improved Machinery Performance using Active Control Technology. BRITE/EURAM Project No. BRPR-CT97-0544, Jan. 1998-March 2001.

[29] Mueller M. (2002) On-line-Process Monitoring in High Speed Milling with an Active Magnetic Bearing Spindle. Diss ETH Zurich, to appear.

[30] R. Field, V. Iannello, A Reliable Magnetic Bearing System for Turbomachinery. *Proc. of the 6th International Symp. on Magnetic Bearings*, MIT Cambridge, 42-51.